

Enhanced photocatalytic activity of ZnO nanoparticles by surface modification with KF using thermal shock method

Le, Tien Khoa; Nguyen, Thi Minh Tram; Nguyen, Huu Thinh Pham; Nguyen, Thi Kieu Loan; Lund, Torben; Nguyen, Huu Khanh Hung; Huynh, Thi Kieu Xuan

Published in:
Arabian Journal of Chemistry

DOI:
[10.1016/j.arabjc.2017.09.006](https://doi.org/10.1016/j.arabjc.2017.09.006)

Publication date:
2020

Document Version
Publisher's PDF, also known as Version of record

Citation for published version (APA):
Le, T. K., Nguyen, T. M. T., Nguyen, H. T. P., Nguyen, T. K. L., Lund, T., Nguyen, H. K. H., & Huynh, T. K. X. (2020). Enhanced photocatalytic activity of ZnO nanoparticles by surface modification with KF using thermal shock method. *Arabian Journal of Chemistry*, 13(1), 1032-1039. <https://doi.org/10.1016/j.arabjc.2017.09.006>

General rights

Copyright and moral rights for the publications made accessible in the public portal are retained by the authors and/or other copyright owners and it is a condition of accessing publications that users recognise and abide by the legal requirements associated with these rights.

- Users may download and print one copy of any publication from the public portal for the purpose of private study or research.
- You may not further distribute the material or use it for any profit-making activity or commercial gain.
- You may freely distribute the URL identifying the publication in the public portal.

Take down policy

If you believe that this document breaches copyright please contact rucforsk@kb.dk providing details, and we will remove access to the work immediately and investigate your claim.



King Saud University
Arabian Journal of Chemistry

www.ksu.edu.sa
www.sciencedirect.com



ORIGINAL ARTICLE

Enhanced photocatalytic activity of ZnO nanoparticles by surface modification with KF using thermal shock method



Tien Khoa Le^a, Thi Minh Tram Nguyen^a, Huu Thinh Pham Nguyen^a,
Thi Kieu Loan Nguyen^a, Torben Lund^b, Huu Khanh Hung Nguyen^a,
Thi Kieu Xuan Huynh^{a,*}

^a University of Science – Vietnam National University HoChiMinh City, 227 Nguyen Van Cu Street, Ho Chi Minh City, Viet Nam

^b Department of Science and Environment, Roskilde University, 4000 Roskilde, Denmark

Received 13 June 2017; accepted 6 September 2017

Available online 14 September 2017

KEYWORDS

ZnO nanoparticles;
Thermal shock;
KF;
Methylene blue;
Photocatalytic activity

Abstract ZnO nanoparticles were modified with KF using thermal shock method at various temperatures in order to improve the photocatalytic activity of ZnO under both UVA and visible light irradiation. The influences of KF-modification on the crystal structure, morphology, UV–visible absorption, specific surface area as well as surface structure of ZnO were respectively characterized by XRD, FE-SEM, UV–Visible diffuse reflectance, N₂ adsorption and XPS spectroscopy. The photocatalytic activity was evaluated via the degradation of methylene blue under UVA irradiation. According to the results, the thermal shock process with KF did not modify the structure, the particle size and the optical properties of ZnO nanoparticles but successfully increase their UVA and visible light induced photocatalytic activity. This enhancement of activity may be attributed to the increase of surface hydroxyl groups and zinc vacancies of modified ZnO samples.

© 2017 The Authors. Production and hosting by Elsevier B.V. on behalf of King Saud University. This is an open access article under the CC BY-NC-ND license (<http://creativecommons.org/licenses/by-nc-nd/4.0/>).

1. Introduction

Although TiO₂ was extensively investigated as the most important and popular photocatalyst, photocatalytic materials based

on ZnO have also attracted increasing attention owing to their comparable band gap energy with TiO₂ (Ye and Ohmori, 2002; Kukreja et al., 2004), higher quantum efficiency and lower cost than TiO₂ (Khodja et al., 2001; Sakthivel et al., 2003). Similar to TiO₂, the drawback of ZnO is its very low activity under visible light (Rehman et al., 2009; Ma et al., 2013). As a consequence, both ZnO and TiO₂ still need to be modified in order to increase its photocatalytic performance. Recently, F-doping in TiO₂ (Yu et al., 2002; Mori et al., 2008; Huo et al., 2009) or ZnO lattice (Kadi et al., 2016; Podporska-Carroll et al., 2017) was considered as one of efficient ways to narrow the band gap of these semiconductors, which is able

* Corresponding author.

E-mail address: htkxuan@hcmus.edu.vn (T.K.X. Huynh).

Peer review under responsibility of King Saud University.



Production and hosting by Elsevier

to increase their UV-light and visible-light-induced photocatalytic activity. However, these structural-doping approaches usually require high-priced titanium and fluorine precursors (titanium isopropoxide (Yu et al., 2009), titanium butoxide (Khodja et al., 2001; Jiang et al., 2007), trifluoroacetic acid (Podporska-Carroll et al., 2017) as well as special techniques with sophisticated devices and operating conditions (sputtering chamber for radio frequency magnetron sputtering (Yoon et al., 2008), three-electrode system for chronoamperometry method (Ilican et al., 2016) and a large amount of solvent for sol-gel method (Podporska-Carroll et al., 2017), which are not suitable for large scale production.

In the other hand, it has been well known that most of photocatalytic processes occur on the oxide surface. Hence, surface modification should be a simple and inexpensive approach to enhance the photocatalytic activity of TiO_2 and ZnO. In fact, several studies reported that the surface of TiO_2 can be modified by a simple ligand exchange between surface hydroxyl groups of TiO_2 and fluoride ions (Minero et al., 2000; Park and Choi, 2004), which was proved to be able to enhance the production of hydroxyl radicals (Vijayabalan et al., 2009). Recently, we also successfully developed a novel, facile and quickly method, thermal shock method, to fluorinate the surface of TiO_2 nanoparticles (Le et al., 2012; Le et al., 2014). This method is based on thermal treatment of TiO_2 at 400–600 °C during a short time (5 min) which allows us to modify the surface of TiO_2 without affecting its bulk structure. It was observed that our thermal shock fluorination method can effectively improve the performance of TiO_2 under both UV and visible light irradiation due to the increase of surface hydroxyl groups and oxygen vacancies. Nevertheless, according to our best knowledge, there is still no report on the surface fluorination of ZnO nanophotocatalysts.

Therefore, surface-modified ZnO nanoparticles with KF by presented thermal shock method at various temperatures to create new photocatalytic materials which present high photocatalytic activity under both UV and visible light irradiation was goal of this paper. The influences of different thermal shock temperatures on the crystal structure, surface structure and morphology as well as photocatalytic performance were also investigated.

2. Experimental section

2.1. Sample preparation

The starting materials $\text{Zn}(\text{CH}_3\text{COO})_2 \cdot 2\text{H}_2\text{O}$, $\text{H}_2\text{C}_2\text{O}_4 \cdot 2\text{H}_2\text{O}$ and KF (99%, extra pure grade) were purchased from Sigma Aldrich. Methylene blue (MB) (analytical grade) was purchased from Merck. These chemicals were used as received without further purification. Distilled water was used in all the experiments. Firstly, ZnO was prepared by a simple precipitation method as follows: 160 mL of $\text{H}_2\text{C}_2\text{O}_4$ solution (0.500 mol L^{-1}) was slowly added to 160 mL of $\text{Zn}(\text{CH}_3\text{COO})_2$ solution (0.500 mol L^{-1}) to form a white slurry solution. The precipitate was filtered and dried at 150 °C during 3 h. Then the solid was annealed at 500 °C for 2 h to obtain ZnO nanoparticles.

Thereafter, our thermal shock method was employed to modify the surface of ZnO with KF agent. ZnO nanoparticles were added in 10 mL of KF solution (0.625 mol L^{-1}) with the

molar ratio of fluorine to zinc of 1:1 under constant magnetic stirring for 30 min. The resulting white suspension was dried at 150 °C during 3 h. Subsequently, the powder was placed in an electric furnace at different temperatures (400, 500 and 600 °C) and rapidly removed from the furnace after 5 min to be cooled down to room temperature. Finally, the sample was washed in distilled water to take off the remained KF on its surface and then dried again at 150 °C for 1 h. In the following manuscript, the KF-modified ZnO samples were labelled as FZnO-X (with X the temperature of thermal shock process).

2.2. Characterization

The phase purity and crystal structure of ZnO and ZnO-X samples were examined by X-ray powder diffraction, measured on a BRUKER-Binary V3 X-ray diffractometer using $\text{Cu K}\alpha$ radiation ($\lambda = 1.5406 \text{ \AA}$). The accelerating voltage and the applied current were 40 kV and 40 mA, respectively. The determination of phase composition was referenced to the Joint Committee on Powder Diffraction Standards (JCPDS cards). The Rietveld refinement was carried out using the Fullprof 2009 structure refinement software (Rodriguez-Carvajal, 2001). Moreover, the crystallite diameter was calculated using the Debye–Scherrer formula from the full width of half maximum of the most intense diffraction peak of ZnO ((1 0 1) line). The morphology and microstructures of these samples were observed by field emission scanning electron microscopy (FE-SEM). Their FE-SEM micrographs were recorded using a HITACHI S-4800 with an acceleration voltage at 10 kV. The Brunauer-Emmet-Teller surface area (S_{BET}) of samples was obtained through a heat pretreatment at 150 °C for 2 h followed by nitrogen adsorption-desorption experiments using a NOVA 1000e analyzer (Quantachrome Instruments). The UV–visible absorption spectra of catalysts were obtained on a Jasco V-550 spectrophotometer (JASCO Corp.) using BaSO_4 as a reference. The surface atomic composition and chemical environment of ZnO and ZnO-X catalysts were characterized by X-ray photoelectron spectroscopy (XPS) measurements on a Kratos Axis Ultra-DLD spectrometer (Kratos Analytical Ltd, UK) equipped with an Al-K α source (1486.6 eV) operating at 150 W in a pressure of 10^{-7} mbar. All the binding energies were referenced to the C1s peak located at 285 eV attributed to the surface contamination carbon.

2.3. Photocatalytic tests

The photocatalytic activities of ZnO and ZnO-X samples were evaluated via the degradation of MB. An aqueous solution of the MB (10^{-5} mol L^{-1} , 250 mL) was taken into the glass reactor covered with aluminium layer which prevents the exterior light and the required amount of photocatalyst (0.5 g L^{-1}) was added. The reactor suspension was stirred continuously by a mechanic agitator and cooled by continuous water flow in order to maintain the suspension temperature at 30 °C during the experiments. The initial pH of suspensions was determined at 7. Before irradiation, the suspension was magnetically stirred in the dark for 60 min to obtain the MB adsorption equilibrium. Then the reaction suspension was irradiated by an Osram 9-W UV light lamp or an Osram 9-W visible light lamp placed about 10 cm above the suspension surface. During the illumination, 5 mL of suspension was col-

lected at regular time intervals and analysed by a UV–visible Helios Omega spectrophotometer.

3. Results and discussion

3.1. Catalyst characterization

The XRD patterns of bare ZnO and KF-modified powders are illustrated in Fig. 1. The spectrum of bare ZnO sample show a series of diffraction peaks at the position of 31.79° ((1 0 0) line), 34.41° ((0 0 2) line), 36.21° ((1 0 1) line), 47.58° ((1 0 2) line), 56.53° ((1 1 0) line) and 62.84° ((1 0 3) line), which is in good agreement with the standard JCPDS file of ZnO zincite phase (space group P6₃mc, JCPDS No. 36-1451). It was observed that surface modification with KF by thermal shock method at various temperatures did not affect the phase composition of ZnO since only peaks corresponding to the zincite phase were found in the XRD patterns of fluorinated samples.

The morphology of bare ZnO and ZnO-400, ZnO-500 and ZnO-600 catalysts was investigated using FE-SEM. The micrographs in Fig. 2a reveal the multi-dispersed particles of bare ZnO sample in agglomerated nanostructure. These particles are mostly hexagonal in shape with the particle size varying from 50 to 150 nm. When ZnO was modified by thermal shock method with KF from 400 to 600 °C (Fig. 2b–d), the size and shape of ZnO particles almost remained unchanged. However, KF-modification seems to slightly increase the crystallite diameter of modified ZnO samples calculated from the Debye–Scherrer formula (Table 1). A minor decrease in BET surface area was also observed for FZnO catalysts prepared at 500–600 °C (Table 1). These evolutions in FZnO-X samples should be attributed to the minor aggregation of ZnO crystals induced by the 5-min-thermal-shock treatment. Nevertheless, these evolutions are not significant, which demonstrated that the crystal structure, crystallite size and specific surface area are not disturbed by our KF-thermal shock method.

The UV–visible absorption spectra of bare ZnO and KF-modified samples are exhibited in Fig. 3. Their band gap values

are also presented in Table 1. Bare ZnO nanoparticles show no absorption in the zone of 450–800 nm but an intense and broad absorption from 200–450 nm with the maximum absorption peak at 372 nm, indicating that ZnO only absorb effectively UV light. It was also seen that the modification process did not affect the optical properties of ZnO since all KF-modified samples show identical UV–visible adsorption spectra and similar band gap values to the bare ZnO sample.

The surface composition and the chemical environment of all elements on the surface of our catalysts were characterized by XPS and reported in Table 2. The C 1s core peaks due to surface contamination carbon presented in all bare ZnO and KF-modified ZnO samples can be deconvoluted into three peaks: the main peak at 285 eV is attributed to C–C and C–H bonds whereas the two lower peaks at 286.6 and 289.0 eV are assigned to Zn–O–C and O=C–O bonds of carbonate species, respectively (Papirer et al., 1995; Sun et al., 2016). Fig. 4 shows the high resolution XPS spectra of the Zn 2p region, taken on the surface of bare ZnO and ZnO-X samples. Due to spin-orbit coupling, each spectrum consists of two main Zn 2p components at the position of 1021.6 (Zn 2p_{3/2}) and 1044.7 eV (Zn 2p_{1/2}). These binding energies are representative of the Zn²⁺ ions in the oxygen environment, which is in good agreement with previous studies (Anandan et al., 2010; Yousef et al., 2012). It was observed that the modification of TiO₂ with KF by thermal shock method does not affect the oxidation state and the chemical environment of zinc atoms at the surface of ZnO. Interestingly, the high resolution XPS spectra for our modified catalysts show no peak in the F 1s region (Fig. 5). It should be reminded that in our previous study, when TiO₂ was fluorinated by thermal shock method, the F 1s core peak was observed at 684.5 eV, which corresponds to the chemisorbed fluoride ions on TiO₂ surface. The absence of this peak in our actual ZnO-X samples suggests that the chemisorption of fluoride ions is not favoured on ZnO surface. In other words, the fluoride ions may loosely bind to surface Zn²⁺ ions, so that they are easily hydrolysed to be removed from the surface and possibly result in certain effects.

The high resolution O 1s spectra (Fig. 6) of bare ZnO, FZnO-400, FZnO-500 and FZnO-600 samples show an asymmetric peak which can be deconvoluted into different components. Generally, in the literature, the O 1s spectra of ZnO may be composed of three components: the first component (O_I) located at ~530 eV corresponding to O²⁻ ions of ZnO lattice (Chen et al., 2000), the second component (O_{II}) at ~531.6 eV attributed to oxygen atoms of hydroxyl groups on the oxide surface (Dupin et al., 2000; Al-Gaashani et al., 2013), and the third component (O_{III}) situated at ~533.2 eV corresponding to water molecules adsorbed on the oxide surface (Ma et al., 2013). Based on these XPS data, it was observed that the XPS O 1s spectra of bare ZnO, FZnO-400 and FZnO-500 samples only include two component peaks: the most intense peak located at 530.4 eV and a minor peak at 531.8 eV attributed to the O_I and O_{II} components, respectively. When ZnO was modified with KF at 600 °C, an additional weak peak appeared at 533.4 eV, which is assigned to the O_{III} component of surface oxygen atoms. Herein, the calculation of O_{II}/Zn and Zn/O_I atomic ratios was carried out to follow the evolution of surface oxygen species due to KF-modification (Table 2). It was observed that the O_{II}/Zn atomic ratio was clearly enhanced when ZnO was modified with KF

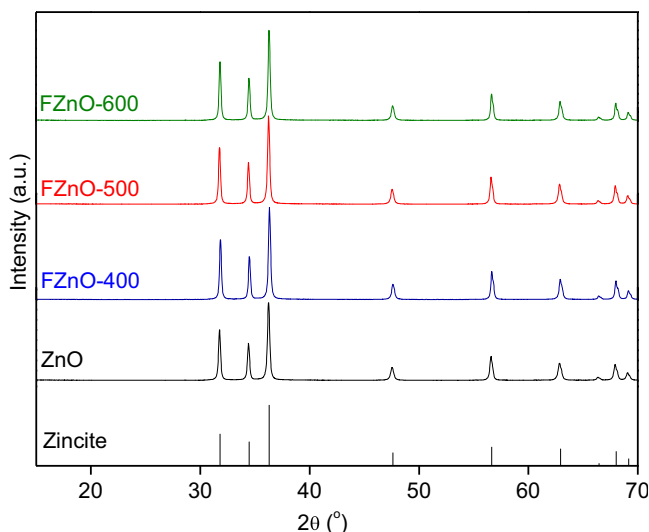


Fig. 1 XRD patterns of bare ZnO and KF-modified ZnO samples (FZnO-400, FZnO-500 and FZnO-600).

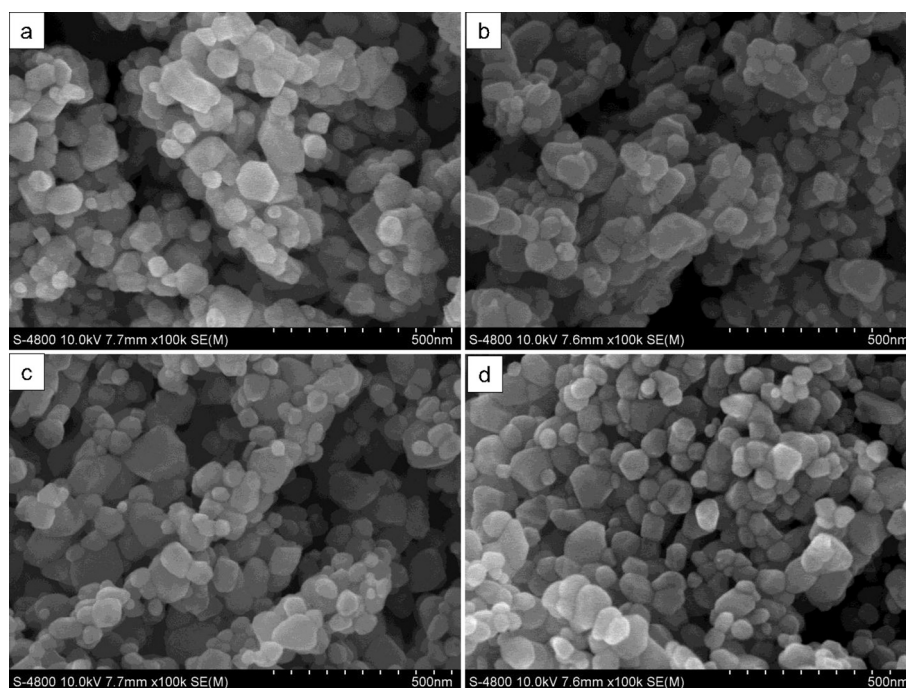


Fig. 2 SEM micrographs of (a) bare ZnO, (b) FZnO-400, (c) FZnO-500 and (d) FZnO-600.

Table 1 Debye–Scherrer crystallite size, BET surface area and band gap values of bare ZnO and KF-modified ZnO samples.

Sample	Debye–Scherrer crystallite size (nm)	BET surface area (m ² /g)	Band gap values (eV)
ZnO	38.62	12.298	3.17
FZnO-400	41.57	12.540	3.19
FZnO-500	41.29	10.500	3.19
FZnO-600	42.08	10.464	3.19

by thermal shock method at 400 and 500 °C, demonstrating the increase of surface hydroxyl groups due to KF-modification by thermal shock method. Moreover, the Zn/O₁ atomic ratio for these samples was lower than 1, the stoichiometric Zn/O₁ atomic ratio of ZnO. This substoichiometry suggests that the thermal shock with KF can form the zinc vacancies on the surface. However, there was a clear decrease in zinc vacancies for FZnO-600 sample, corresponding to the increase of Zn/O₁ atomic ratio.

3.2. Photocatalytic activity

The UVA light and visible light induced photocatalytic activities of bare ZnO and ZnO-X samples were evaluated via the photocatalytic MB degradation. Figs. 7 and 8 show the time-dependent profiles of MB degradation in the presence of our catalysts under UVA light irradiation and visible light irradiation, respectively. In these figures, all the plots of $\ln(C/C_0)$ versus time (C is the MB concentration at time t and C_0 is the initial MB concentration) are mostly linear, proving that the kinetics of photocatalytic MB decomposition can be described by the pseudo-first-order Langmuir-Hinshelwood kinetic model. Table 3 presents the apparent first-order rate constant

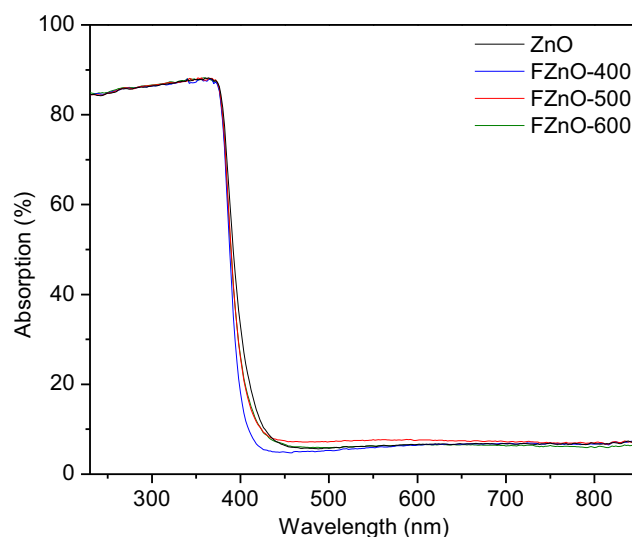
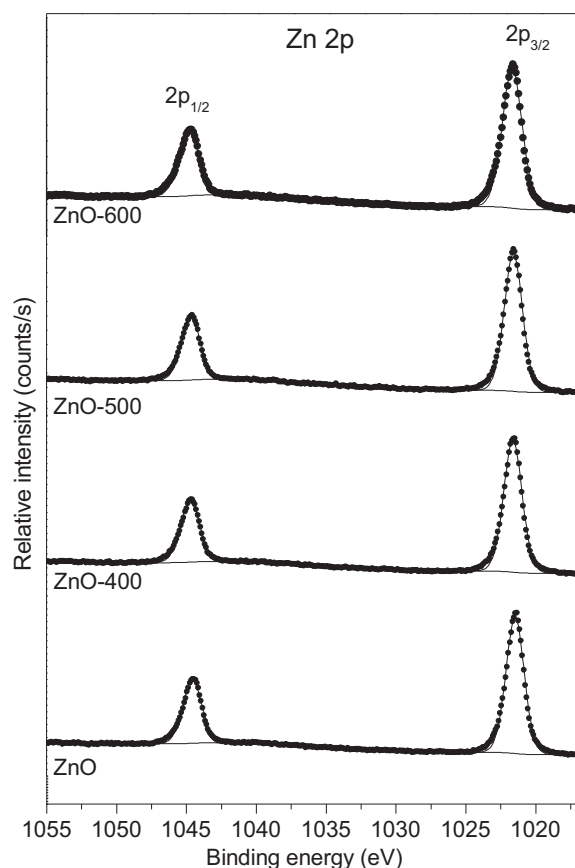


Fig. 3 UV–visible absorption spectra of bare ZnO and KF-modified ZnO samples (FZnO-400, FZnO-500 and FZnO-600).

(k) of MB degradation for our catalysts under UVA and visible light. It can be seen that bare ZnO sample only operated under UVA light ($k = 1.556 \text{ h}^{-1}$) and showed very low activity under visible light ($k = 0.095 \text{ h}^{-1}$). When ZnO was fluorinated at 400 °C and 500 °C, the photocatalytic performance was remarkably improved. The FZnO-500 sample was found to be the best catalyst with the MB degradation rate constant enhanced by the factor of 2.19 ($k = 2.969 \text{ h}^{-1}$) and 3.29 ($k = 0.2253 \text{ h}^{-1}$) under UVA and visible light irradiation, respectively. In the literature, ZnO was doped with different elements for the MB degradation under UV light, such as iron ($k = 0.780 \text{ h}^{-1}$) (Afifah et al., 2015) or yttrium ($k = 2.664 \text{ h}^{-1}$)

Table 2 High resolution XPS data of bare ZnO and KF-modified ZnO samples.

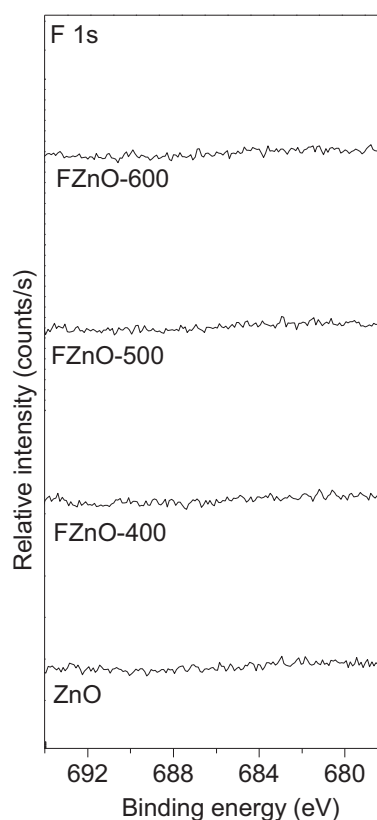
		C1s			Zn2p _{3/2-1/2}	O1s I	O1s II	O1s III	Zn/O _I	O _{II} /Zn
ZnO	B.E. eV	285.0	287	289.0	1021.4–1044.5	530.2	531.8		1.00	0.41
	%	13.00	1.94	2.38	34.32	34.33	14.03			
FZnO-400	B.E. eV	285.0	286.6	289.0	1021.6–1044.7	530.4	531.8		0.94	0.46
	%	15.25	2.42	2.45	31.74	33.66	14.48			
FZnO-500	B.E. eV	285.0	286.7	289.2	1021.6–1044.7	530.4	531.8		0.93	0.44
	%	17.42	2.66	2.48	30.80	33.04	13.62			
FZnO-600	B.E. eV	285.0	286.8	289.2	1021.7–1044.8	530.4	531.8	533.4	0.97	0.57
	%	13.23	1.94	1.42	31.16	32.16	17.88	2.21		

**Fig. 4** High resolution XPS Zn 2p spectra of bare ZnO and KF-modified ZnO samples.

(Sanoop et al., 2016). The higher activity of our FZnO-500 sample confirmed the effectivity of KF-modification by our thermal shock method at 500 °C. However, when the fluorination thermal shock temperature was up to 600 °C, the catalytic activity was decreased under both UVA and visible light.

3.3. Discussion

The evolution of both UVA and visible light induced photocatalytic activity of unmodified and modified ZnO samples (FZnO-400, FZnO-500 and FZnO-600) should be related to the modifications of surface composition since the characterization processes showed no evolution in their phase composi-

**Fig. 5** High resolution XPS F 1s spectra of and KF-modified ZnO samples.

tion, optical properties and particle size. More especially, the XPS studies proved the absence of fluoride species on the surface of FZnO-X samples. These results suggest that during the fluorination at different thermal shock temperatures, fluoride ions may break the oxo-bridges on ZnO surface to form adjacent Zn–F and Zn–O[−] bonds. When our catalysts were washed by distilled water after the thermal shock process, these bonds could be hydrolysed, which created surface hydroxyl groups and removed fluoride ions on the surface. In our previous study (Le et al., 2012), surface fluorination of TiO₂ P25 by thermal shock method successfully created chemisorbed fluoride ions on the oxide surface, which suggests that fluoride ions are more favoured on the TiO₂ surface than ZnO surface. This phenomenon may be explained by the difference of bonding

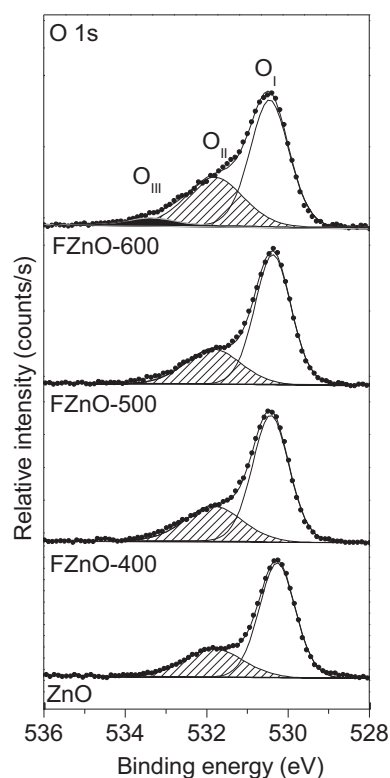


Fig. 6 High resolution XPS O 1s spectra of bare ZnO and KF-modified ZnO samples.

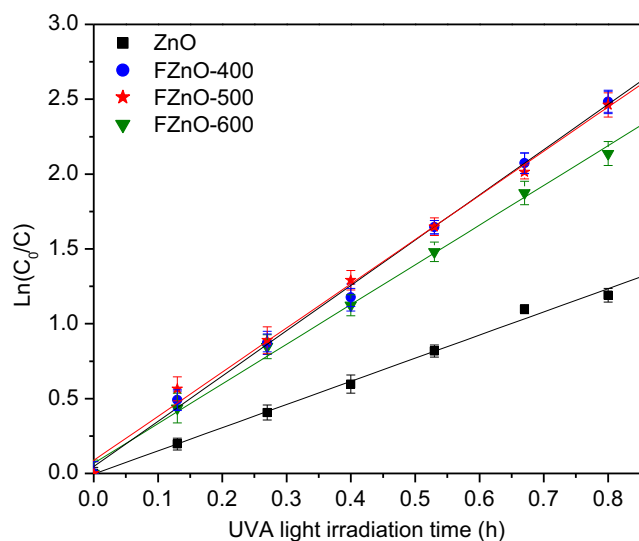


Fig. 7 $\ln(C_0/C)$ versus time plot of MB degradation under UV irradiation on bare ZnO and KF-modified ZnO samples. C is the MB concentration (mol L^{-1}) at time t and C_0 is the initial MB concentration (mol L^{-1}).

energy between Zn-F ($364 \pm 63 \text{ kJ mol}^{-1}$) (Luo, 2007) and Ti-F ($569 \pm 33 \text{ kJ mol}^{-1}$) (Luo, 2007). The higher energy of Ti-F bond allows fluoride ions to remain on the surface of TiO_2 after washed by distilled water. Therefore, three modified FZnO-X samples did not present surface fluoride ions but enhanced surface hydroxyl groups in the comparison with bare

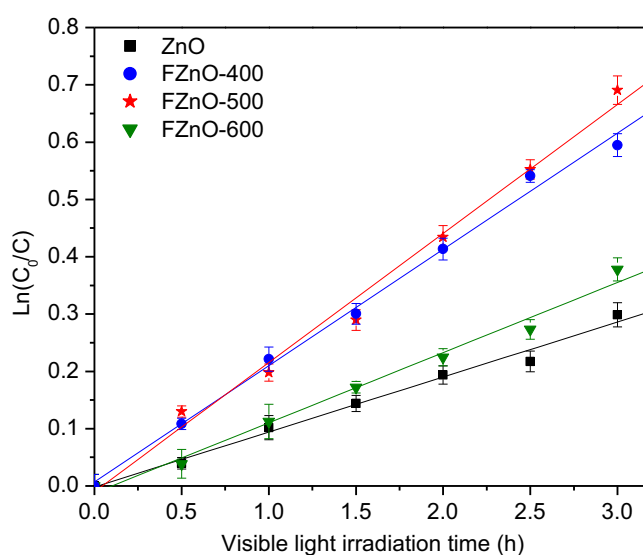


Fig. 8 $\ln(C_0/C)$ versus time plot of MB degradation under visible irradiation on bare ZnO and KF-modified ZnO samples. C is the MB concentration (mol L^{-1}) at time t and C_0 is the initial MB concentration (mol L^{-1}).

Table 3 Comparison of MB degradation rate constant on bare ZnO and KF-modified ZnO catalysts under UVA and visible light irradiation.

Sample	Rate constant of MB degradation under UV illumination (h^{-1})	Rate constant of MB degradation under Visible illumination (h^{-1})
ZnO	1.549	0.0959
FZnO-400	3.035	0.2030
FZnO-500	2.969	0.2253
FZnO-600	2.653	0.1223

ZnO sample. It was reported that most of hydroxyl radicals are formed on the surface of semiconductor oxide via the reaction between surface hydroxyl groups and photogenerated holes (Minero et al., 2000; Minero et al., 2000). Hence, the rise of surface hydroxyl groups on our catalysts modified from 400 to 500 $^{\circ}\text{C}$ is supposed to increase the content of hydroxyl radicals and then the photocatalytic activity, which was also observed in our previous thermal shock fluorinated TiO_2 (Le et al., 2012; Le et al., 2014). However, when the thermal shock temperature was up to 600 $^{\circ}\text{C}$, despite the fact that the content of surface hydroxyl groups still increased, the photocatalytic activity was decreased. Thus this decline in activity should be explained by other factors.

In the other hand, the XPS experiments demonstrated the surface substoichiometric ratios of zinc to lattice oxygen atoms for KF-modified catalysts. Besides, the atomic absorption spectroscopy experiment using a Shimadzu AA-6300 spectrometer (wavelength of 213.9 nm) confirmed the existence of zinc ions with the concentration of about 11.76 ppm in the washing solution of thermal shock process for FZnO-500 whereas very few zinc ions (0.19 ppm) were observed in the washing solution of ZnO preparation. These results proposes that when breaking oxo-bridges, fluorides ions may take off a certain amount of surface zinc ions via the formation of sol-

uble coordination compounds, leading to the generation of zinc vacancies on the surface of FZnO-X samples. Although the effects of oxygen vacancies on the photocatalytic activity have been well reported in the literature (Li et al., 2005; Lachheb et al., 2002; Ho et al., 2006), the role of cation vacancies, especially zinc vacancies was rarely studied. The formation of zinc vacancies may lead to the apparition of neighbouring oxygen atoms with excess valence electrons, which can generate new energetic bands. Recently, using DFT calculations, Pan et al. prevailed the appearance of new transition band above the top of valence band followed by the generation of zinc vacancies (Pan et al., 2014). This band can induce the visible light absorption of ZnO and consequently improve the photocatalytic activity under both UVA and visible light irradiation. Hence, for ZnO catalysts modified with KF by thermal shock at 400–500 °C, the presence of zinc vacancies and the increase of hydroxyl groups on its surface are the main factors enhancing its photocatalytic performance. However, when the thermal shock temperature reached 600 °C, the reduction of zinc vacancies on the surface of FZnO-600 sample was observed, which suggests that high temperatures (from 600 °C) may hinder the formation of soluble coordination compounds between fluoride ions and zinc atoms on the surface of ZnO. Consequently, the photocatalytic activity of FZnO-600 under both UVA and visible light was clearly declined.

4. Conclusion

In this study, ZnO nanoparticles were modified with KF by thermal shock method at various temperatures in order to study the effects of KF-modification on their crystal structure, morphology, optical properties, surface structure and photocatalytic activity. The experimental results show that this modification method does not affect the crystal structure, particle size and optical properties of ZnO but successfully increases the surface hydroxyl groups and zinc vacancies, which result in the enhancement of UVA and visible light induced response. The ZnO catalyst modified with KF at 500 °C was found to be the best photocatalyst with the activity enhanced by the factor of 2.19 (under UVA light) and 3.29 (under visible light) in comparison with bare ZnO nanoparticles. These results indicated that our simple thermal shock method combined with KF can effectively modify the surface of ZnO nanoparticles, leading to the improvement of their photocatalytic performance.

Acknowledgments

This research is funded by Vietnam National University HoChiMinh City (VNU-HCM) under grant number B2017-18-08.

The authors acknowledge The World Academy of Sciences (TWAS) for their supports under grant number 15-106 RG/CHE/AS_G – FR3240287033.

References

Ye, F.X., Ohmori, A., 2002. The photocatalytic activity and photoabsorption of plasma sprayed $\text{TiO}_2\text{-Fe}_3\text{O}_4$ binary oxide coatings. *Surf. Coat. Technol.* 160, 62–67.

- Kukreja, L.M., Barik, S., Misra, P., 2004. Variable band gap ZnO nanostructures grown by pulsed laser deposition. *J. Cryst. Growth* 268, 531–535.
- Khodja, A.A., Sehili, T., Pilichowski, J.F., Boule, P., 2001. Photocatalytic degradation of 2-phenylphenol on TiO_2 and ZnO in aqueous suspensions. *J. Photochem. Photobiol. A* 141, 231–239.
- Sakthivel, S., Neppolian, B., Shankar, M.V., Arabindoo, B., Palanichamy, M., Murugesan, V., 2003. Solar photocatalytic degradation of azo dye: comparison of photocatalytic efficiency of ZnO and TiO_2 . *Sol. Energy Mater. Sol. Cells* 77, 65–82.
- Rehman, S., Ullah, R., Butt, A.M., Gohar, N.D., 2009. Strategies of making TiO_2 and ZnO visible light active. *J. Hazard. Mater.* 170, 560–569.
- Ma, H., Cheng, X., Ma, C., Dong, X., Zhang, X., Xue, M., Zhang, X., Fu, Y., 2013. Synthesis, characterization and photocatalytic activity of N-Doped ZnO/ZnS composites. *Int. J. Photoenergy* 2013, 1–8.
- Yu, J.C., Yu, J., Ho, W., Jiang, Z., Zhang, L., 2002. Effects of F[−] doping on the photocatalytic activity and microstructures of nanocrystalline TiO_2 powders. *Chem. Mater.* 14, 3808–3816.
- Mori, K., Maki, K., Kawasaki, S., Yuan, S., Yamashita, H., 2008. Hydrothermal synthesis of TiO_2 photocatalysts in the presence of NH_4F and their application for degradation of organic compounds. *Chem. Eng. Sci.* 63, 5066–5070.
- Huo, Y., Jin, Y., Zhu, J., Li, H., 2009. Highly active $\text{TiO}_{2-x}\text{N}_x\text{F}_y$ visible photocatalyst prepared under supercritical conditions in $\text{NH}_4\text{F}/\text{EtOH}$ fluid. *Appl. Catal. B: Environ.* 89, 543–550.
- Kadi, M.V., David McKinney, D., Mohammed, R.M., Mkhaliid, I.A., Sigmund, W., 2016. Fluorine doped zinc oxide nanowires: enhanced photocatalysts degrade malachite green dye under visible light conditions. *Ceram. Int.* 42, 4672–4678.
- Podporska-Carroll, J., Myles, A., Quilty, B., McCormack, D., Fagan, R., Hinder, S., Dionysiou, D.D., Pillai, S., 2017. Antibacterial properties of F-doped ZnO visible light photocatalyst. *J. Hazard. Mater.* 324, 39–47.
- Yu, C., Yu, J.C., Chan, M., 2009. Sonochemical fabrication of fluorinated mesoporous titanium dioxide microspheres. *J. Solid State Chem.* 182, 1061–1069.
- Jiang, H., Song, H., Zhou, Z., Liu, X., Meng, G., 2007. The roles of Li⁺ and F[−] ions in Li-F-codoped TiO_2 system. *J. Phys. Chem. Solids* 68, 1830–1835.
- Yoon, H.S., Lee, K.S., Lee, T.S., Cheong, B., Choi, D.K., Kim, D.H., Kim, W.M., 2008. Properties of fluorine doped ZnO thin films deposited by magnetron sputtering. *Sol. Energy Mater. Sol. Cells* 92, 1366–1372.
- Ilican, S., Caglar, M., Aksoy, S., Caglar, Y., 2016. XPS studies of electrodeposited grown F-doped ZnO rods and electrical properties of p-Si/n-FZN heterojunctions. *J. Nanomater.* 2016, 1–9.
- Minero, C., Mariella, G., Maurino, V., Vione, D., Pelizzetti, E., 2000. Photocatalytic transformation of organic compounds in the presence of inorganic ions. 2. Competitive reactions of phenol and alcohols on a titanium dioxide-fluoride system. *Langmuir* 16, 8964–8972.
- Park, H., Choi, W., 2004. Effects of TiO_2 surface fluorination on photocatalytic reactions and photoelectrochemical behaviors. *J. Phys. Chem. B* 108, 4086–4093.
- Vijayabalan, A., Selvam, K., Velmurugan, R., Swaminathan, M., 2009. Photocatalytic activity of surface fluorinated $\text{TiO}_2\text{-P25}$ in the degradation of reactive orange 4. *J. Hazard. Mater.* 172, 914–921.
- Le, T.K., Flahaut, D., Foix, D., Blanc, S., Nguyen, H.K.H., Huynh, T.K.X., Martinez, H., 2012. Study of surface fluorination of photocatalytic TiO_2 by thermal shock method. *J. Solid State Chem.* 187, 300–308.
- Le, T.K., Flahaut, D., Martinez, H., Pigot, T., Nguyen, H.K.H., Huynh, T.K.X., 2014. Surface fluorination of single-phase TiO_2 by thermal shock method for enhanced UV and visible light induced photocatalytic activity. *Appl. Catal. B: Environ.* 144, 1–11.

- Rodriguez-Carvajal, J., 2001. Recent developments of the program FULLPROF, commission of powder diffraction. IUCr Newslett. 26, 12–19.
- Papirer, E., Lacroix, R., Donnet, J.B., Nansé, G., Fioux, P., 1995. XPS study of the halogenation of carbon black – Part 2. Chlorination. Carbon 33, 63–72.
- Sun, H.Q., Bai, Y., Cheng, Y.P., Jin, W.Q., Xu, N.P., 2016. Preparation and characterization of visible-light-driven carbon-sulfur-codoped TiO₂ photocatalysts. Ind. Eng. Chem. Res. 45, 4971–4976.
- Anandan, S., Ohashi, N., Miyauchi, M., 2010. ZnO-based visible-light photocatalyst: band-gap engineering and multi-electron reduction by co-catalyst. Appl. Catal. B: Environ. 100, 502–509.
- Yousef, A., Barakat, N.A.M., Amna, T., Unnithan, A.R., Al-Deyab, S.S., Kim, H.Y., 2012. Influence of CdO-doping on the photoluminescence properties of ZnO nanofibers: effective visible light photocatalyst for waste water treatment. J. Lumin. 132, 1668–1677.
- Chen, M., Wang, X., Yu, Y., Pei, Z., Bai, X., Sun, C., Huang, R.F., Wen, L.S., 2000. X-ray photoelectron spectroscopy and auger electron spectroscopy studies of Al-doped ZnO films. Appl. Surf. Sci. 158, 134–140.
- Dupin, J.C., Gonbeau, D., Vinatier, P., Levasseur, A., 2000. Systematic XPS studies of metal oxides, hydroxides and peroxides. Phys. Chem. Chem. Phys. 2, 1319.
- Al-Gaashani, R., Radiman, S., Daud, A., Tabet, N., Al-Douri, Y., 2013. XPS and optical studies of different morphologies of ZnO nanostructures prepared by microwave methods. Ceram. Int. 39, 2283–2292.
- Afifah, N., Adriani, S., Djaja, N.F., Saleh, R., 2015. Photocatalytic degradation of methylene blue and methyl orange with Fe-doped ZnO nanoparticles modified with natural zeolite and montmorillonite: comparative study. Adv. Mater. Res. 1123, 295–302.
- Sanoop, P.K., Anas, S., Ananthakumar, S., Gunasekar, V., Saravanan, R., Ponnusami, V., 2016. Synthesis of yttrium doped nanocrystalline ZnO and its photocatalytic activity in methylene blue degradation. Arab. J. Chem. 9, S1618–S1626.
- Luo, Y.R., 2007. Comprehensive Handbook of Chemical Bond Energies. CRC Press, Boca Raton, FL.
- Minero, C., Mariella, G., Maurino, V., Vione, D., Pelizzetti, E., 2000. Photocatalytic transformation of organic compounds in the presence of inorganic anions. I. Hydroxyl-mediated and direct electron-transfer reactions of phenol on a titanium dioxide–fluoride system. Langmuir 16, 2632–2641.
- Li, D., Ohashi, N., Hishita, S., Kolodiazny, T., Haneda, H., 2005. Origin of visible-light-driven photocatalysis: a comparative study on N/F-doped and N-F-codoped TiO₂ powders by means of experimental characterizations and theoretical calculations. J. Solid State Chem. 178, 3293–3302.
- Lachheb, H., Puzeat, E., Houas, A., Ksibi, M., Elaloui, E., Guillard, C., Herrmann, J.M., 2002. Photocatalytic degradation of various types of dyes (Alizarin S, Crocein Orange G, Methyl Red, Congo Red, Methylene Blue) in water by UV-irradiated titania. Appl. Catal. B 39, 75–90.
- Ho, W., Yu, J.C., Lee, S., 2006. Synthesis of hierarchical nanoporous F-doped TiO₂ spheres with visible light photocatalytic activity. Chem. Commun. 10, 1115–1117.
- Pan, L., Wang, S., Mi, W., Song, J., Zou, J., Wang, L., Zhang, X., 2014. Undoped ZnO abundant with metal vacancies. Nano Energ. 9, 71–79.